Evaluation of Stirling cooler system for cryogenic CO_2 capture

Chun Feng Song, Yutaka Kitamura*, Shu Hong Li

Graduate School of Life and Environmental Sciences, University of Tsukuba, 1-1-1, Tennodai, Tsukuba, Ibaraki 305-8572, Japan

* Corresponding author. Tel.: +81 0298-53-4655; Fax: +81 0298-53-4655.

E-mail address: kitamura.yutaka.fm@u.tsukuba.ac.jp

Abstract

In previous research, a cryogenic system based on Stirling coolers has been developed. In this work, the novel system was applied on CO_2 capture from post-combustion flue gas and different process parameters (*i.e.* flow rate of feed gas, temperature of Stirling cooler and operating condition) were investigated to obtain the optimal performance (CO_2 recovery and energy consumption). From the extensive experiments, it was concluded that the cryogenic system could realize CO_2 capture without solvent and pressure drop condition. Meanwhile, the results showed that for post-combustion, the novel SC system can capture above 80% CO_2 from flue gas with 3.4 MJ/kg CO_2.

Keywords*:* CO_2 capture, cryogenic, Stirling cooler, CO_2 recovery, energy consumption

1. Introduction

Due to the issue of greenhouse effect getting more serious, it is of great importance to develop an optimal technology for greenhouse gas (GHG) control. Meanwhile, as a main part of GHG, CO_2 capture and storage (CCS) from large sources, such as coal-fired power plants, is considered as a viable approach to reduce GHG emissions. In the foreseeable future (up to 2050), most countries around the world, especially emerging countries with rich coal resources, will still use fossil energy as their primary energy resource [1]. For example, China currently generates 80% of its power by burning coal, while India obtains more than two-thirds of its electricity from coal and Germany and the United States use it for approximately one-half of their power needs [2]. Nowadays, the main CO_2 capture technologies are: post-combustion, pre-combustion and oxy-fuel combustion [3].

Among the technologies for reduction of CO_2 emissions, post-combustion technology is most likely to be commercialized and used in most existing coal-fired power plant [4]. Post-combustion capture: In this case, the CO_2 is separated from the flue gas emitted after

the combustion of fossil fuels (from a standard gas turbine combined cycle or a coal-fired steam power plant) [5]. CO_2 separation is realized at the relatively high temperature, from a gaseous stream at atmospheric pressure and with low CO_2 concentration (typically 10-15 vol.%) [6]. This possibility is by far the most challenging since a diluted, low pressure, hot and wet CO_2/N_2 mixture has to be treated. Although oxy-fuel and pre-combustion technologies are studied extensively to be applied into to-be-built power plants, post-combustion also corresponds to the most widely applicable option for retrofitting existing industrial sectors (*e.g.* power plants, cement, kiln and steel production) [7,8].

Various processes can be envisaged for post-combustion CO_2 capture. They are based on: 1) Chemical absorption. Nowadays, the dominated solvent used for absorption is amines. The advantages of chemical technologies are that can be implemented at atmospheric pressure and used to capture low partial pressure CO_2 from flue gas in coal-fired power plants [9-11]. 2) Physical adsorption. As an alternative technology for CO_2 capture, two dominant adsorption processes can be available, *viz.* temperature swing adsorption (TSA) and pressure/vacuum swing adsorption (PSA/VSA). Taking the advantages of the adsorption processes, a high CO_2 purity can be achieved. However, the main drawback is low productivity, which results in large adsorbent amount [12-14]. 3) Membranes separation. In the past few years, there has been a remarkable development in membrane separation for CO_2 capture from flue gas. The major interest of membrane

permeation techniques concerns the possibility to significantly decrease the size of the capture installation and environment friendly. The primary limitation for membrane techniques is the high capital cost of raw materials. Meanwhile, the energy cost of generating the required pressure difference across the membrane is also a key issue [15,16].

4) Cryogenic anti-sublimation. Cryogenic CO_2 capture techniques can realize CO_2 capture without the energy penalty of solvent regeneration and pressure drop generation. Nevertheless, the cryogenic capture process covers a large range of operating condition from normal to supercritical state, and involves multi-components in flue gas (typically as CO_2, N_2, O_2, H_2O, NO_x, and SO_x). So far, the current technologies can not satisfy the requirements of the commercial application [17-20]. Although the existing technologies such as liquid scrubbing are available for CO_2 capture from flue gas, the cost of capture is still too high. Cost (capital and operating) becomes the major barrier to the application of CO_2 capture in power plant and other CO_2 emission industry sectors. Therefore, most of the researchers focus on improving of CO_2 capture efficiency and decreasing the energy penalty. The target of energy consumption is as low as possible (around 1 MJ/kg CO_2) while keeping high CO_2 recovery (above 90%) [21].

As an alternative technology, previous feasibility studies on the application of cryogenic CO_2 capture processes for their use in post-combustion processes suggest that principally CO_2 can be removed from flue gas [22,23]. Although for the past years, this technology

was not extensively studied due to the expected expensive cooling cost, in fact, the CO_2 capture efficiency (at 1 atmosphere) of the cryogenic capture process can reach 99% at -135 °C and 90% at -120 °C [24]. By comparison, most existing processes are not reasonably capable of achieving 99% CO_2 capture. Moreover, the CO_2 captured with a cryogenic process has virtually no impurity in it. In 2002, Clodic and Younes [25] developed a cryogenic CO_2 capture process, where CO_2 was desublimated as a solid onto surfaces of heat exchangers, which were cooled by evaporating a refrigerants blend. The energy requirement of the whole process was in the range of 541 to 1119 kJ/kg CO_2 [26], which could compete with the other post combustion technologies. Nevertheless, the disadvantage of this method is that moisture in feed gas should be removed in order to avoid plugging in the system. In addition, the method of taking off the increasing layer of dry ice onto heat exchanger surfaces during the capture process was not introduced, which would adversely affect the heat transfer and reduce the capture efficiency. In 2010, Tuinier et al. [27] exploited a novel cryogenic CO_2 capture process using dynamically operated packed beds. By the developed process above 99% CO_2 can be recovered from a flue gas containing 10 vol.% CO_2 and 1 vol.% H_2O with 1.8 MJ/kg CO_2 energy consumption.

In the previous work, a novel CO_2 capture process based on Stirling coolers (SCs) has been demonstrated [28]. The aim of this study is to apply the exploited cryogenic system on CO_2 capture of post-combustion and evaluate the capture performance. To achieve this

objective, a variation of several parameters has been investigated. The varied parameters include: the condition of the capture process, the flow rate of gas stream and the temperature of SC-1. Furthermore, a comparison between the novel process and the existing post-combustion CO_2 capture technologies has also been implemented.

2. Description of the novel system

2.1 Cryogenic CO_2 capture process

The schematic of the cryogenic capture process is shown in Fig.1. The main parts contain SCs, vacuum pump, freezing tower, camera and control panel. The whole process is composed of three stages: refrigeration, capture and storage.

2.1.1 Refrigeration by SC-1

Firstly, feed gas is cooled from 25 °C to 0 °C by SC-1 in the pre-freezing tower. At the pre-freezing tower, the moisture in feed gas condenses into water by SC-1 and then moves through the condenser pipe to the outlet to avoid plugging the vessel, which is the key issue of cryogenic separation technology. Meanwhile, the other gas flows into the main-freezing tower.

2.1.2 Capture by SC-2

In the main-freezing tower, SC-2 provides a cryogenic condition (approximately -100 ~

-105 °C), and the flue gas after water removed is cooled down to about -100 °C. In this condition, CO_2 in flue gas (about 15 vol.%) desublimates into the solid form, which has a frost point of -100 °C [29]. Afterwards, the dry ice frosts onto the heat exchanger of SC-2 immediately. In this way, the capture of CO_2 from feed gas is realized.

2.1.3 Storage by SC-3

The last step is to store the solid CO_2 by SC-3. In this section, by spinning the scraping rod on the cooling fin of SC-2 heat exchanger, dry ice falls down to the storage tank, where SC-3 provides a cryogenic condition (below -78.5 °C) to prevent it gasifying. On the other hand, residual gas exhausts from gas outlet.

2.2 Numerical model of the frost process

In order to deepen the understanding of capture characteristic and improve the capture efficiency, the CO_2 frost formation process was simulated in this section. The process was described by a numerical model. The frost formation process involves simultaneous heat and mass transfer during varying thermo physical properties. To simplify the complex process, some assumptions were employed: 1) Frost layer distribution is homogeneous over the cooling fin; 2) The frosting process takes place at a quasi-steady state; 3) Frost thermal conductivity of the frost layer varies only with frost density; 4) Radiation heat transfer between flue gas and frost layer is negligible. The structure in the main freezing tower and

the direction of airflow has been described in Fig 2(a), and the temperature distribution in the main freezing tower has been simulated in Fig 2(b). The detail description of the simulation process can be found in the previous work [28].

From the mass balance of frost, the increase of frost layer per unit surface area (M_s) is determined from:

$$\frac{dM_s}{dt} = m_t \tag{1}$$

where m_t is the mass flux of CO_2 deposition from flue gas to the surface of cooling fin, and it can be obtained in terms of:

$$m_t = h_{m,co_2}(\rho_{co_2,g} - \rho_{co_2,s}) \tag{2}$$

where $h_{m,CO2}$ is the mass transfer coefficient of solid CO_2; $\rho co_{2,g}$ and $\rho co_{2,s}$ are the densities of CO_2 in flue gas and frost surface, respectively. Since the CO_2 gas is assumed to be an ideal gas, $\rho co_{2,g}$ and $\rho co_{2,s}$ can be calculated from the following equations of states [30]:

$$\rho_{CO_2,g} = \frac{\omega P_{sat,g}}{R_{CO_2} T_g} \tag{3}$$

$$\rho_{CO_2,s} = \frac{P_{sat,s}}{R_{CO_2} T_s} \tag{4}$$

where ω is the percentage composition of CO_2 in flue gas. T_g and T_s are the temperature of flue gas and frost surface, severally. $P_{sat,g}$ and $P_{sat,s}$ denote the saturation pressure of CO_2 at T_g and T_s, respectively, and R_{CO2} is the gas constant of CO_2. In addition, the frost layer thickness (δ_f) on cooling fin surface of SC-2 heat exchanger is calculated as:

$$\delta_f = \frac{M_s}{\rho_{co_2,s}} \tag{5}$$

where $\rho co_{2,s}$ is the density of frost layer.

In order to describe the influence of heat transfer, the effective thermal conductivity of frost layer (k_f) is introduced, and the heat balance at cooling fin surface of SC-2 heat exchanger is determined from:

$$k_f \frac{T_f - T_g}{\delta_f} = Q \tag{6}$$

where Q is the total heat flux to the frost layer and is equal to the sum of heat fluxes by convection (Q_c) and phase change (Q_p) as following:

$$Q = Q_c + Q_p \tag{7}$$

The convective heat transfer can be calculated by the equations described by [31]:

$$Q_c = h_c (T_g - T_f) \tag{8}$$

$$h_c = \left| h_{nc}^3 + h_{fc}^3 \right|^{1/3} \tag{9}$$

$$h_{nc} = \frac{k_g \cdot Nu_{nc}}{L} \tag{10}$$

$$h_{fc} = \frac{k_g \cdot Nu_{fc}}{D} \tag{11}$$

$$Nu_{nc} = \left\{ 0.825 + \frac{0.387 Ra^{1/6}}{\left[1 + \left(0.492 / Pr \right)^{9/16} \right]^{8/27}} \right\}^2 \tag{12}$$

$$Nu_{fc} = 0.3 + \frac{0.62 Re^{2/3} Pr^{1/3}}{\left[1+\left(0.4/Pr\right)^{2/3}\right]^{1/4}} \left[1+\left(\frac{Re}{282.000}\right)^{5/8}\right]^{4/5} \quad (13)$$

where h_{nc} and h_{fc} denote the heat transfer coefficients of natural and forced convection, respectively. k_g is the effective thermal conductivity of the gas stream. *Nu* is Nusselt number, *Ra* is Rayleigh number, *Pr* is Prandtl number and *Re* is Reynolds number.

The phase-change heat transfer is equal to:

$$Q_p = m_t q \quad (14)$$

where q is the latent heat of sublimation, which has been estimated by [32]:

$$q = 2.88 \times 10^6 - 195 T_f \quad (15)$$

3. Experimental

3.1 Experiments

The structure of the whole system is shown in Fig. 3. The detail layout of the apparatus has been presented in the previous work [28]. The flue gas of post-combustion was simulated by syngas (87% N_2 and 13% CO_2). Meanwhile, no pollutants in flue gas such as SO_x and NO_x was assumed.

In addition, it is noteworthy that the materials selection of structure should be adjusted to taking into consideration of the effect on cryogenic performance. The materials used for experimental setup are stainless steel. The material of heat transfer heads is copper, which

has a relative ideal coefficient for heat transfer. The joint between the cold head of SCs and freezing tower are wrapped up by thermal insulating materials to reduce heat loss as much as possible. Due to some synthetic materials may become ineffective in low temperature condition, specific sealing materials and gaskets (low temperature resistant, approximately -120 °C) are necessarily required for the pipe fittings to avoid the gas leakage of the system.

3.2 Performance parameters

As the key parameters to represent the performance of CO_2 capture process, CO_2 capture efficiency and energy consumption were investigated in this research. According to ideal gas equation and definition of density:

$$PV = nRT \tag{16}$$

$$\rho = \frac{M}{V} \tag{17}$$

it can be concluded that:

$$\rho_{CO_2,in} = \frac{M_{CO_2}}{V_{CO_2,in}} = \frac{M_{CO_2}}{\frac{nRT_{in}}{P_{in}}} \tag{18}$$

$$\rho_{CO_2,out} = \frac{M_{CO_2}}{V_{CO_2,out}} = \frac{M_{CO_2}}{\frac{nRT_{out}}{P_{out}}} \tag{19}$$

Hence, the CO_2 capture efficiency is defined as:

$$\eta_{CO_2\ recovery} = 1 - \frac{v_{out}\omega_{CO_2,out}P_{out}T_{in}}{v_{in}\omega_{CO_2,in}P_{in}T_{out}} \qquad [\%] \tag{20}$$

where η is CO_2 capture efficiency; v is flow rate of gas mixture and ω is percentage of CO_2 in gas mixture. In addition, the subscripts *in* and *out* represent the state of inlet and outlet, respectively.

The energy consumption (EC) of the cryogenic system for per unit mass CO_2 captured is defined as following:

$$\mathrm{EC} = \frac{UI}{\left(\frac{v_{in}\omega_{CO_2,in}P_{in}}{T_{in}} - \frac{v_{out}\omega_{CO_2,out}P_{out}}{T_{out}}\right)} \cdot \frac{nR}{M_{CO_2}} \qquad [MJ / kg\ CO_2] \tag{21}$$

in which U and I are voltage and current in the system, respectively. v_{in} and v_{out} are the volume flow rates of gas mixture at inlet and outlet.

4. Results and discussion

4.1 Effect of processing conditions

4.1.1 Effect of evacuation pressure

First, the performance of the cryogenic capture process with and without vacuum evacuation was investigated. While linked with a vacuum pump, the interlayer vacuum degree of the system is approximately 2 hPa (depended on the capacity of vacuum pump, Nakamura Seisakusho Co., Ltd.); while without vacuum pump, the pressure is the

atmosphere (1.01×10^5 Pa).

Fig. 4 shows the effect of evacuation pressure on the temperature variation of the process, and the results show that the effect of vacuum condition is mainly on the temperature of SC-1, and either with or without vacuum pump the temperature of SC-2 and 3 changes a little. That can be explained by the fact that due to an existing interlayer in the pre-freezing tower, an evacuated condition of the interlayer is conducive to create a thermal insulation layer to prevent heat transfer from ambient to inside, and to effectively keep the cryogenic condition in the system. Besides, in Fig. 5, when the system is connected with a vacuum pump, the energy consumption is lower, and the variation of CO_2 recovery is not significant. For energy consumption, vacuum condition reduced thermal loss to decrease energy penalty. By contrast, since the CO_2 capture and storage proceed by SC-2 and 3, the evacuation condition had no significant influence on CO_2 recovery.

4.1.2 Effect of operating time

In this section, the influence of operating time on the performance of the system has been investigated. It should be pointed out that operating time of the whole process is comprised by two parts, idle operating time and capture time. Hereinto, idle operating time is defined as the runtime of the system before flue gas inflow, and its aim is to generate the required cryogenic condition (under the frost point of CO_2) for the next capture section; capture time denotes the working time when the system captures CO_2. Since the capture time is a

constant for different experiments in this research, idle operating time is set as the parameter that affects capture performance, and it was set as 3 h, 4 h and 5 h, respectively. Besides, the capture time is always 20 minutes.

According to the experiment of operating time (see Fig. 6), the system performance is not improved with increasing the running time straightly. Considering to both capture efficiency and energy consumption, the optimal operating time for the system is 4 h (which has high capture efficiency and low energy consumption). Thus, for the future test, the operating time is selected as 4 h.

4.2 Effect of flow rate

In the section, the evolution of the energy consumption and CO_2 recovery has been tested as a function of flow rate of the flue gas. The flow rate of feed gas was varied to obtain the optimum value with minimal energy consumption and maximal CO_2 recovery.

In Fig. 7 and 8, it indicates that as the flow rate of feed gas increases from 1 to 2 L/min, energy consumption of the system decreases obviously but CO_2 recovery is generally consistent. That is due to that the distribution of temperature presents a decline trend from the interior to exterior in the main-freezing tower, which has been numerically simulated in section 2.2. As a result, the cooling fin of SC-2 has the lowest temperature. Consequently, in order to improve capture efficiency, the gas stream should pass through the cold head of SC-2 as much as possible. When the flow rate is set as 2 L/min, the volume flux of feed gas

passed through the cooling fin per second is greater than 1 and 1.5 L/min, and it is lower energy consumption for per unit of CO_2 captured. Simultaneously, due to the variation flow rate (1 to 2 L/min) is moderate, no significant change is found on CO_2 recovery. Thus, in the case of 2 L/min, the performance of the system is the best among three different flow rates.

4.3 Effect of temperature of SC-1

Finally, the effect of different temperature of SC-1 on the performance of cryogenic CO_2 capture has also been investigated, and the temperature of SC-1 was varied from -60 °C to -20 °C.

From the result in Fig. 9, when the gas stream flows into the system at the beginning stage, the energy consumption of per unit captured CO_2 is high. With time passes (after 10 minutes), the energy penalty decreases and remains stability. Meanwhile, for the same flow rate, when the temperature of SC-1 increases from -60 °C to -20 °C, energy consumption decreases obviously. It is attributed that the function of SC-1 is to chill the feed gas and separate moisture, and this objective can be achieved when the temperature of SC-1 is set to -20 °C. Therefore, in the case of -20 °C of SC-1, the energy consumption of the capture process is low. For CO_2 recovery (shown in Fig. 10), it increases rapidly at the initial 10 minutes. After that, the rate of growth gradually reduces until equilibrium. That can be explained by the fact that at the initial stage of gas inflow, the temperature of the cold head

is low enough to capture CO_2 from flue gas. With time passes, the frosted CO_2 on the heat exchanger would adversely affect the heat transfer process, and this phenomenon led to the decrease of the growing rate of CO_2 capture efficiency until to an equilibrium. Under the flow rate of 2 L/min and temperature of SC-1 of -20 °C, the CO_2 recovery can achieve 85%. Through the test of temperature of SC-1, we obtain the conclusion that it is not obviously regular for the effect of temperature of SC-1 on capture efficiency, and yet for energy consumption, the higher temperature, the lower energy consumption.

4.4 Comparison with existing CO_2 capture technologies

The capture efficiency and energy penalty of the developed cryogenic CO_2 capture system was compared to other technologies in this section. Prior to the comparison, it needs to be noted that for different technologies the types of requirement energy are also different. For amine absorption techniques, two parts of the energy should be considered. One is the thermal energy used for solvent regeneration, which dominates the energy penalty of the whole process. The other small part is the electrical energy to the operation of the installations. For thermal swing adsorption (TSA), the process can be directly heat driven through the jacket. For membrane separation, all the energy required is electrical energy to generate a pressure drop. For the process in this work, the cryogenic condition and operation of the system are both based on the electrical energy consumption. In addition, for the mentioned technologies, the compression energy of CO_2 transport and storage

should also be considered. As a consequence, in order to make a significant comparison, the capital investment and capture condition are primarily investigated. The details of the comparison are listed in Table 1. The results indicate that the capital investment and energy penalty of the membrane process is the highest among the technologies, which is due to its expensive material and energy requirement for permeation under the flue gas condition. By contrast, the present cryogenic capture system can effectively reduce the energy penalty of CO_2 capture with a recovery above 80%. It indicates that as a promising process for CO_2 capture, the novel system based on SCs is worth investigating.

5. Conclusions

In this work, the performance of the cryogenic CO_2 capture system based on SCs has been evaluated. The effect of parameters (such as flow rate, temperature, vacuum condition and operating time) on capture efficiency and energy consumption were investigated. According to the evaluation results, the conclusions can be summarized as follows:

(1) Operating conditions (vacuum condition of the interlayer, operating time of the installation, flow rate of gas stream and temperature of SC-1) dramatically influence the capture efficiency and energy consumption of the novel cryogenic CO_2 capture system. Experimental results show that under the condition (with a vacuum pump, idle operating time of 4 h, flow rate of 2 L/min and temperature of

SC-1 of -20 °C), the global process accomplishes 85% CO_2 recovery with 3.4 MJ/kg CO_2 consumption.

(2) Compared to the existing technologies, the novel cryogenic CO_2 capture process based on Stirling coolers is a promising alternative. The main advantage of the system is to realize CO_2 capture at atmosphere pressure and avoid the regeneration of solvent and energy penalty of pressure drop. Moreover, small-scale installation and environment friendly are also competitive. However, there still have several drawbacks that need to overcome for the novel SC based process. First, it takes a long idle operating time for the required cryogenic condition. Second, the frost layer of captured CO_2 will adversely affect the heat transfer and reduce the overall efficiency.

(3) In the future work, the improvement of the cryogenic CO_2 capture system will be implemented through retrofitting the equipment and enhancing thermal isolation. Furthermore, although the evaluation result of the novel SC system is helpful in the improvement of the CO_2 capture process, it still stays in the laboratory stage. Therefore, a pilot plant test should be carried out in the next work.

Acknowledgement

The authors acknowledge the funding provided by Japan Science and Technology

Agency (JST). We thank Mr. Yamano and Mr. Yamasaki of Tanabe Engineering Corporation for their help on technology.

References

[1] Intetnational Energy Agency (IEA). CO_2 Capture and storage-a key carbon abatement option. OECD/IEA. Paris; 2008.

[2] Hoffmann BS, Szklo A. Integrated gasification combined cycle and carbon capture: A risky option to mitigate CO_2 emissions of coal-fired power plants. Appl Energy 2011;88:3917-29.

[3] Kunze C, Spliethoff H. Assessment of oxy-fuel, pre- and post-combustion-based carbon capture for future IGCC plants. Appl Energy 2012;94:109-16.

[4] Huang B, Xu SS, Gao SW, Liu LB, Tao JY, Niu HW, Cai M, Cheng J. Industrial test and techno-economic analysis of CO_2 capture in Huaneng Beijing coal-fired power station. Appl Energy 2010;87:3347-54.

[5] Kanniche M, Bonnivard RG, Jaud P, Marcos JV, Amann JM, Bouallou C. Pre-combustion, post-combustion and oxy-combustion in thermal power plant for CO_2 capture. Appl Therm Eng 2010;30:53-62.

[6] Favre E. Carbon dioxide recovery from post-combustion processes: can gas permeation membranes compete with absorption? J Membrane Sci 2007;294:50-59.

[7] Hetland J, Kvamsdal HM, Haugen G, Major F, Kaarstad V, Tjellander G. Integrating a full carbon

capture scheme onto a 450 MWe NGCC electric power generation hub for offshore operations: Presenting the Sevan GTW concept. Appl Energy 2009;86:2298-307.

[8] Mokhtar M, Ali MT, Khalilpour R, Abbas A, Shah N, Hajaj AA, Armstrong P, Chiesa M, Sgouridis S. Solar-assisted Post-combustion Carbon Capture feasibility study. Appl Energy 2012;92:668-76.

[9] Sun R, Li Y, Liu H, Wu S, Lu C. CO_2 capture performance of calcium-based sorbent doped with manganese salts during calcium looping cycle. Appl Energy 2012;89:368-73.

[10] Abu-Zahra MRM, Schneiders LHJ, Niederer JPM, Feron PHM, Versteeg GF. CO_2 capture from power plant Part I. A parametric study of the technical performance based on monoethanolamine. Int J Greenhouse Gas Control 2007;1:37-46.

[11] Li H, Ditaranto M, Yan J. Carbon capture with low energy penalty: Supplementary fired natural gas combined cycles. Appl Energy (2012), doi:10.1016/j.apenergy.2011.12.034.

[12] Grande CA, Rodrigues AE. Electric Swing Adsorption for CO_2 removal from flue gases. Int J Greenhouse Gas Control 2008;2:194-202.

[13] An H, Feng B, Su S. CO_2 capture by electrothermal swing adsorption with activated carbon fibre materials. Int J Greenhouse Gas Control 2011;5:16-25.

[14] Li H, Jakobsen JP, Wilhelmsen Ø, Yan J. PVTxy properties of CO_2 mixtures relevant for CO_2 capture, transport and storage: Review of available experimental data and theoretical models. Appl Energy 2011;88:3567-79.

[15] Favre E. Membrane processes and postcombustion carbon dioxide capture: Challenges and prospects. Chem Eng J 2011;171:782-93.

[16] Brunetti A, Scura F, Barbieri G, Drioli E. Membrane technologies for CO_2 separation. J Membrane Sci 2010;359:115-25.

[17] Tuinier MJ, Annaland MVS, Kuipers JAM. A novel process for cryogenic CO_2 capture using dynamically operated packed beds-An experimental and numerical study. Int J Greenhouse Gas Control 2011;5:694-701.

[18] Martelli E, Kreutz T, Carbo M, Consonni S, Jansen D. Shell coal IGCCS with carbon capture: Conventional gas quench vs. innovative configurations. Appl Energy 2011;88:3978-89.

[19] Li H, Yan J. Evaluating cubic equations of state for calculation of vapor–liquid equilibrium of CO_2 and CO_2-mixtures for CO_2 capture and storage processes. Appl Energy 2009;86:826-36.

[20] Li H, Yan J. Impacts of equations of state (EOS) and impurities on the volume calculation of CO_2 mixtures in the applications of CO_2 capture and storage (CCS) processes. Appl Energy 2009;86:2760-70.

[21] Clausse M, Merel J, Meunier F. Numerical parametric study on CO_2 capture by indirect thermal swing adsorption. Int J Greenhouse Gas Control 2011;5:206-13.

[22] Hart A, Gnanendran N. Cryogenic CO_2 Capture in Natural Gas. Energy Procedia 2009;1: 697-706.

[23] Chiesa P, Campanari S, Manzolini G. CO_2 cryogenic separation from combined cycles integrated with molten carbonate fuel cells. Int J Hydrogen Energy 2011; 36:10355-65.

[24] Baxter L, Baxter A, Burt S. Cryogenic CO_2 Capture as a Cost-Effective CO_2 Capture Process. International Pittsburgh Coal Conference. Pittsburgh, PA. 2009.

[25] Clodic D, Younes M. A new method for CO_2 capture: frosting CO_2 at atmospheric pressure. Sixth International Conference on Greenhouse Gas Control Technologies, GHGT6, Kyoto, Japan, 1-4 October 2002, pp.155-160.

[26] Clodic D, Younes M, Bill A. Test results of CO_2 capture by anti-sublimation Capture efficiency and energy consumption for Boiler plants. Seventh International Conference on Greenhouse Gas control Technologies GHGT7, Vancouver, Canada, 2004;6-9.

[27] Tuinier MJ, Annaland MVS, Kramer GJ, Kuipers JAM. Cryogenic CO_2 capture using dynamically operated packed beds. Chem Eng Sci 2010;65:114-9.

[28] Song CF, Kitamura Y, Li SH, Ogasawara KJ. Design of a cryogenic CO_2 capture system based on Stirling coolers. Int J Greenhouse Gas Control 2012;7:107-14.

[29] Clodic D, Hitti ER, Younes M, Bill A. CO_2 capture by anti-sublimation Thermo-economic process evaluation.4th Annual Conference on Carbon Capture & Sequestration, Alexandria (VA), USA. May 2-5, 2005.

[30] Kim KH, Ko HJ, Kim K, Kim YW, Cho KJ. Analysis of heat transfer and frost layer formation on a cryogenic tank wall exposed to the humid atmospheric air. Appl Therm Eng 2009;29:2072-9.

[31] Cengel YA, Heat Transfer: A Practical Approach, second ed., McGraw-Hill, 2003.

[32] Fossa M, Tanda G. Study of free convection frost formation on a vertical plate, Exp Therm Fluid

Sci 2002;26:661-8.

[33] Rubin ES. Integrated Environmental Control Model. Center for Energy and Environmental Studies, Carnegie Mellon University, Pittsburgh. 2010.

[34] Merkel TC, Lin H, Wei X, Baker R. Power plant post-combustion carbon dioxide capture: an opportunity for membranes. J Membrane Sci 2010;359:126–39.

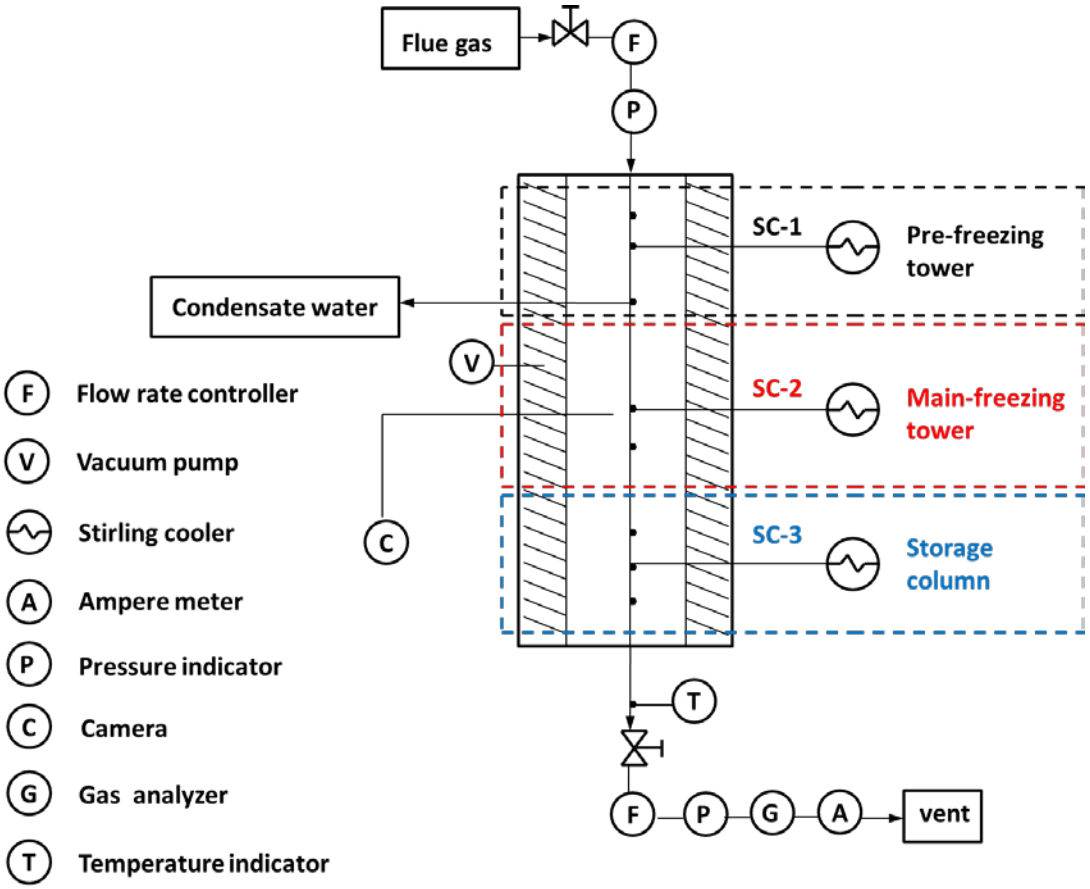

Fig. 1. Schematic of the cryogenic CO_2 capture process based on SCs (represents vacuum area).

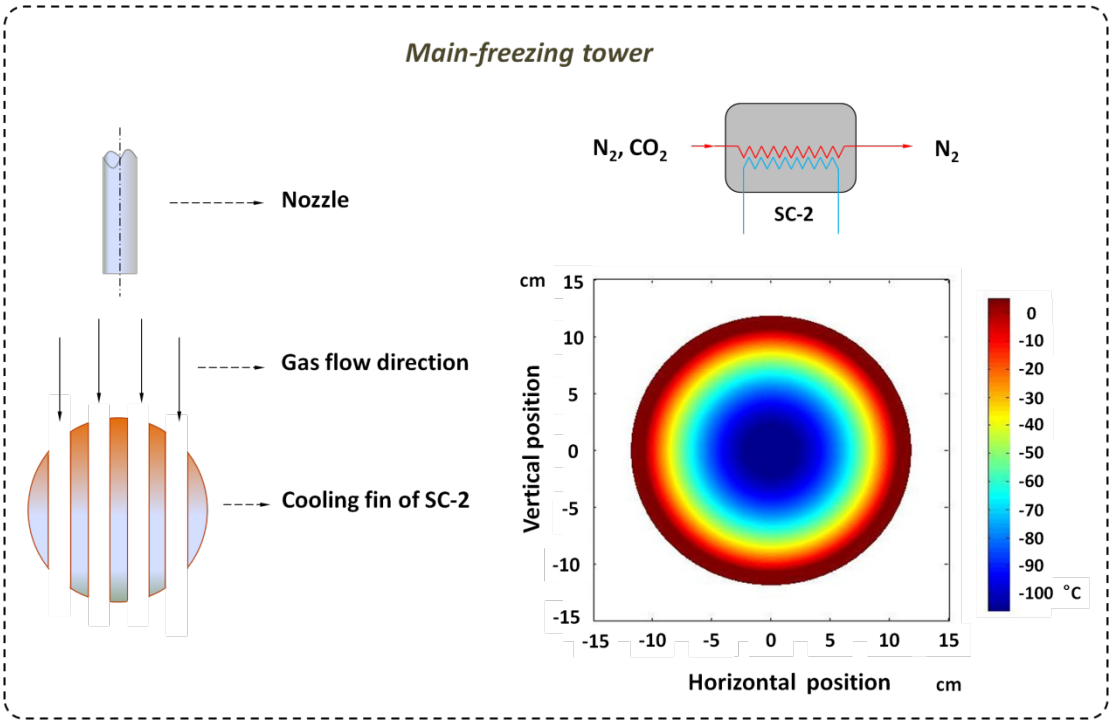

(a) (b)

Fig. 2. The structure and temperature distribution in the main freezing tower.

Fig. 3. Structure of the experiment apparatus.

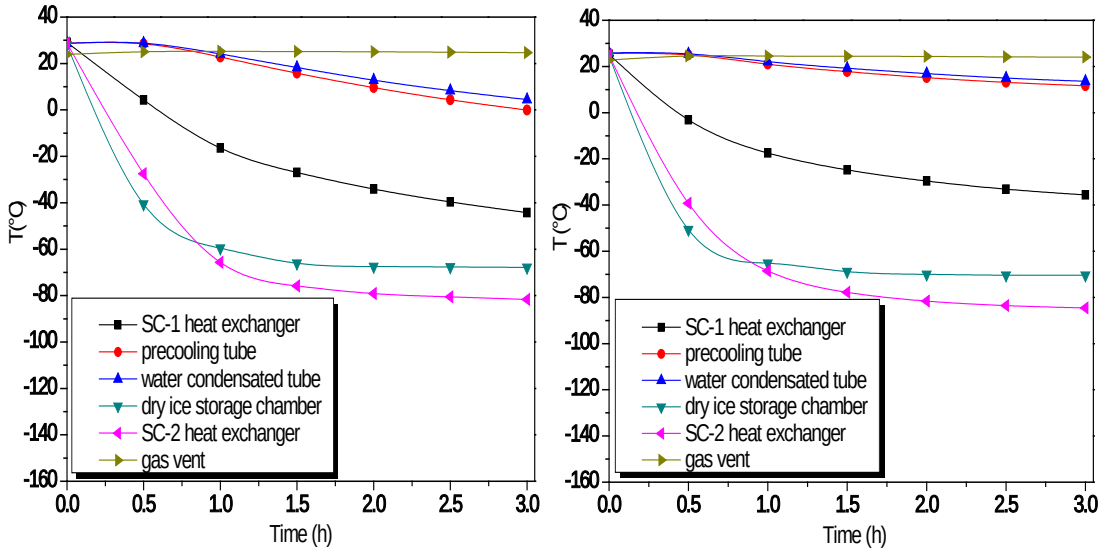

(a) (b)

Fig. 4. Temperature variation in the cryogenic CO_2 capture system with the conjunction of a vacuum pump (a) and without (b) a vacuum pump (T_{sc-1}= -60 °C; T_{sc-2}= -120 °C; T_{sc-3}= -90 °C).

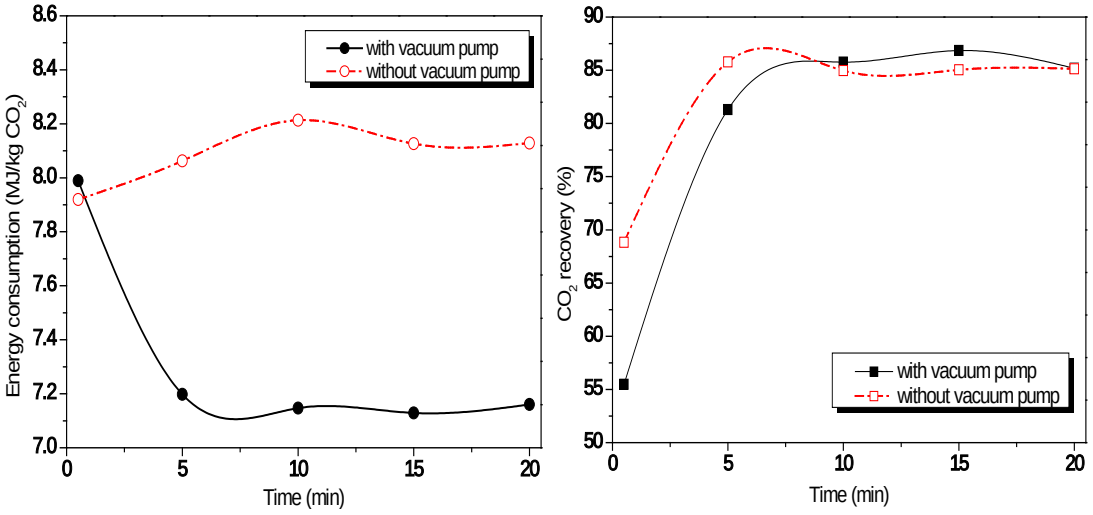

(a) (b)

Fig. 5. The variation of energy consumption (EC) (a) and CO_2 capture efficiency (η) (b) with the conjunction of a vacuum pump and without a vacuum pump(T_{sc-1}= -60 °C; T_{sc-2}= -120 °C; T_{sc-3}= -90 °C; v_{in}=1.5 L/min).

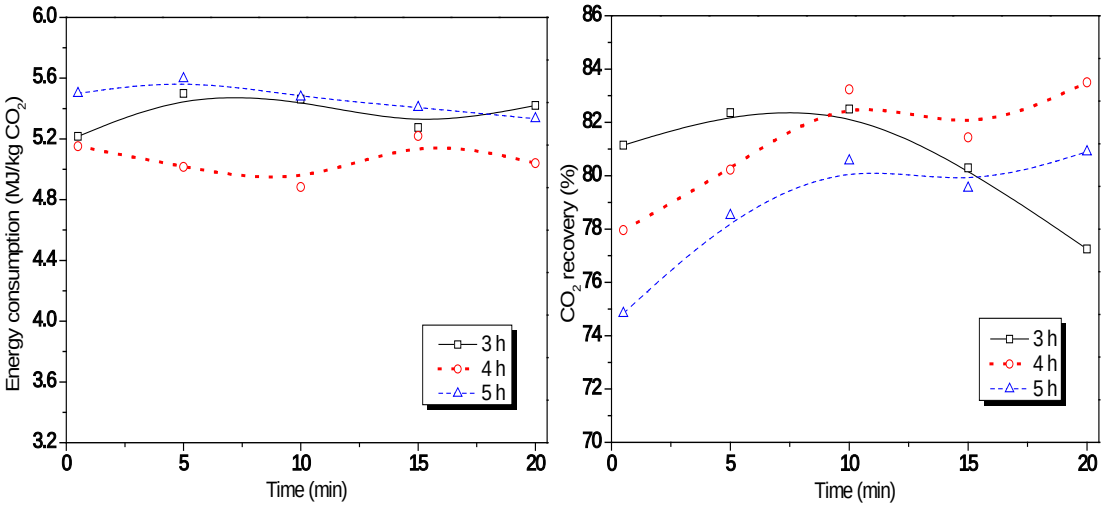

(a) (b)

Fig. 6. Effect of idle operating time (h) of the system on energy consumption (MJ/kg CO_2) (a) and CO_2 capture efficiency (%) (b) (T_{sc-1}= -60 °C; T_{sc-2}= -120 °C; T_{sc-3}= -90 °C; v_{in}=2 L/min).

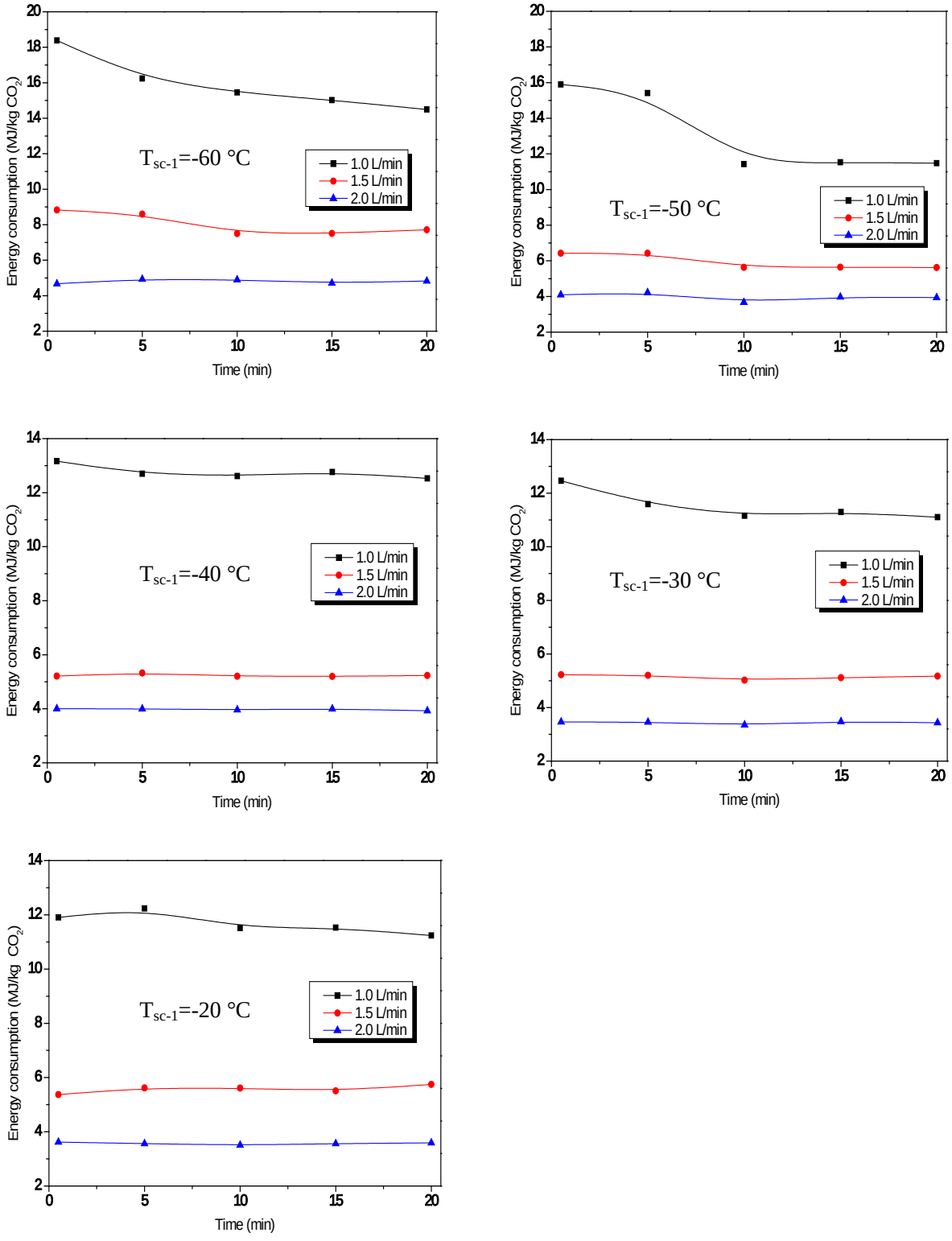

Fig. 7. Energy consumption (EC) at various temperatures (T) of SC-1 for different flow rates (*v*).

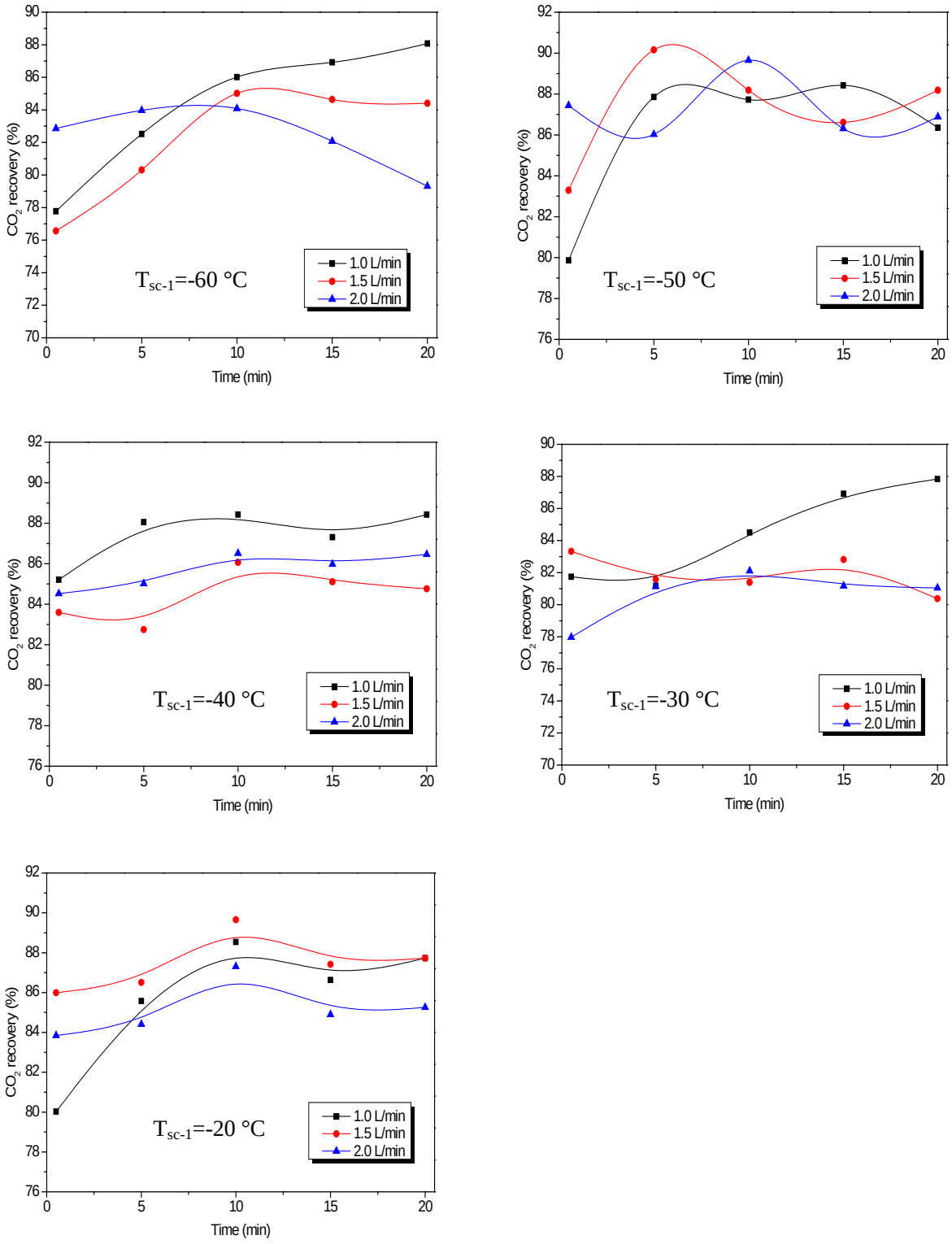

Fig. 8. CO_2 capture efficiency (η) at various temperatures (T) of SC-1 for different flow rates (v).

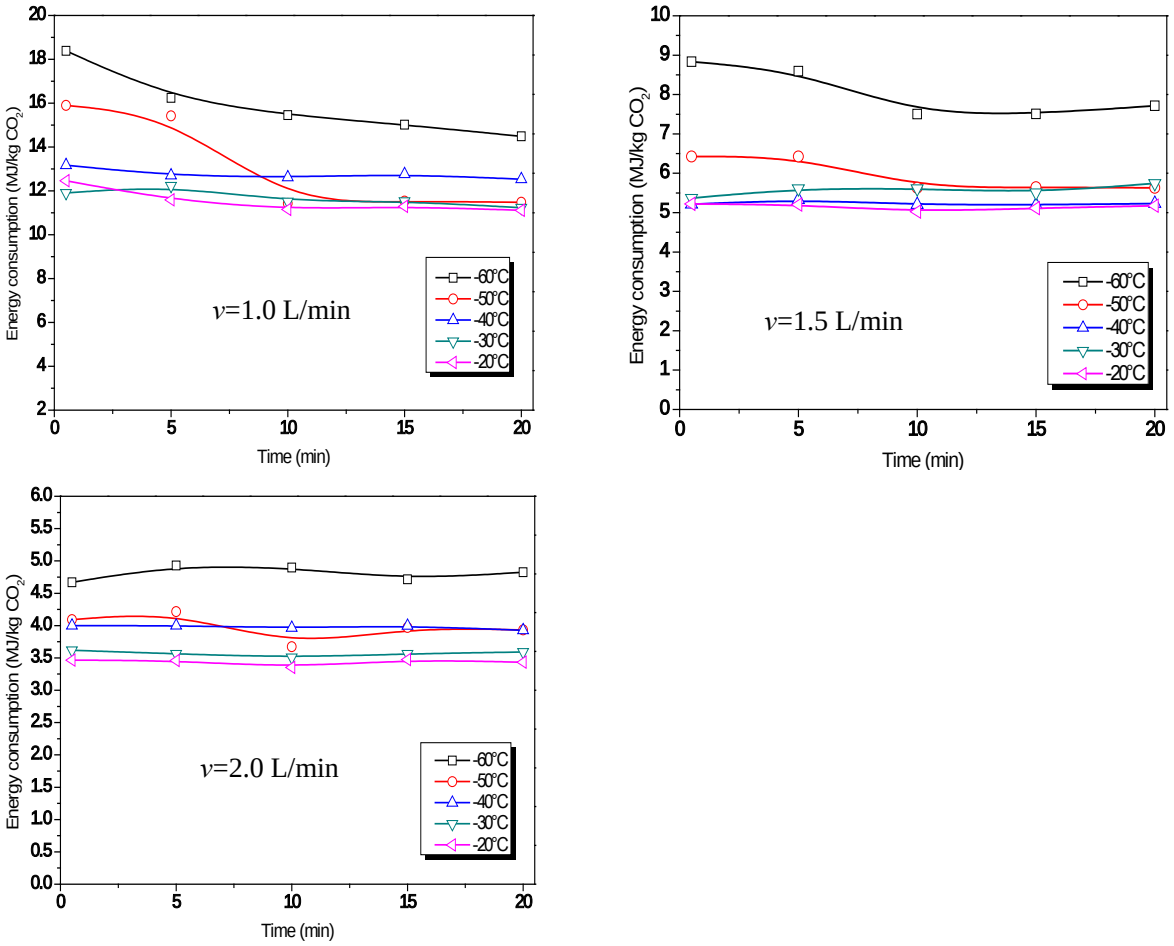

Fig. 9. Energy consumption (EC) at various flow rates (v) for different temperatures (T) of SC-1.

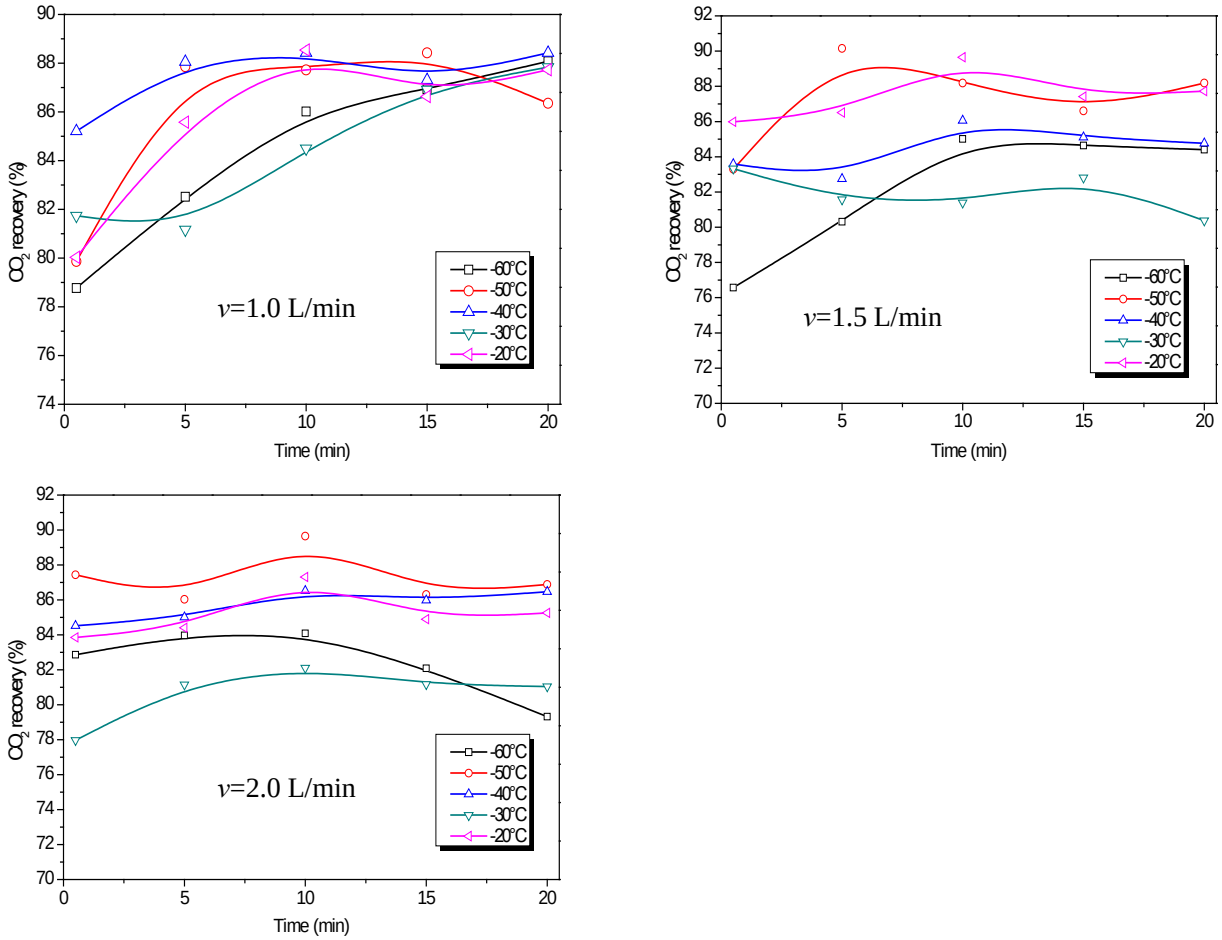

Fig. 10. CO_2 capture efficiency (η) at various flow rates (v) for different temperatures (T) of SC-1.

Table 1

Comparison of the capital investment, capture condition and performance among the dominant technologies [a].

	Amine absorption [33]	Membrane [34]	TSA [b] [21]	The present work
Capital investment (M$)				
Total direct investment	229.3	500	-	0.064
Total allocated investment	119.7	200	-	-
Start up investment	15	25	-	-
Working capital	8.7	15	-	-

Total fixed capital	442.7	740	-	0.07
Capture condition				
Temperature (°C)	-	30	20	25
Flow rate (kg/s)	666	602	0.67	0.07
Composition (vol.%)				
N_2	86	87	90	87
CO_2	14	13	10	13
H_2O	-	-	-	-
O_2	-	-	-	-
Capture performance				
CO_2 productivity (kg CO_2/h)	4.39×10^5	369×10^5	41.5	70.1
Total costs ($/kg CO_2)	0.055	0.121	-	0.052
Total efficiency (% LHV)	35	35	-	-
Efficiency penalty (% LHV basis)	9	24	-	-
CO_2 recovery (%)	88.3	90	81	85
Energy penalty [c]	2.94	3.51	3.23	3.4

[a] The base cases considered for amine absorption and membrane processes are simulated flue gas in 600MW power plants.

The base cases of TSA and present work are simulated syngas in laboratory scale.

[b] TSA is the thermal swing adsorption process.

[c] The specific energy penalty of CO_2 capture for amine and TSA processes is MJ $_{thermal.}$/kg CO_2, and for membrane process and the present work is MJ $_{electrical.}$/kg CO_2.